American Mineralogist, Volume 88, pages 596–603, 2003

Quantitative 3D measurement of ilmenite abundance in Alpe Arami olivine by confocal microscopy: Confirmation of high-pressure origin

KRASSIMIR N. BOZHILOV,* HARRY W. GREEN II, AND LARISSA F. DOBRZHINETSKAYA

Institute of Geophysics and Planetary Physics and Department of Earth Sciences, University of California, Riverside, California 92521, U.S.A.

ABSTRACT

A critical aspect of the debate about the origin and conditions of metamorphism of the Alpe Arami (AA) peridotite is the disagreement over how much ilmenite is contained in the older generation of olivine and therefore how much TiO_2 might have been dissolved at high pressure and temperature. We have now determined quantitatively the 3-dimensional distribution of ilmenite in AA olivine by confocal laser scanning microscopy (CLSM). The CLSM measurements show an average concentration of 0.31 vol% of ilmenite in olivine, with individual grains containing up to 1.2 vol%. This translates into average and maximum concentrations of 0.23 and 0.9 wt% TiO_2 in olivine, respectively, and confirms the original estimation of maximum concentration of ~1 vol% TiO_2. The vast majority of ilmenite in AA olivine is distributed randomly (although topotactically oriented) and, in all cases, is accompanied by chromite in a ratio of ~4:1. These observations are consistent with an origin of the ilmenite (and chromite) by exsolution from an olivine solid solution at P = 9–12 GPa and temperatures above the stability field of titanian clinohumite, but are not consistent with suggested breakdown of titanian clinohumite. Combining these results with other recent findings suggests that exsolution followed deformation under relatively high fugacity of H_2O, and that the high solubility of TiO_2 is probably explained by pressure-induced accommodation of Ti in the tetrahedral site of silicates.

INTRODUCTION

The origin of the garnet lherzolite of the Alpe Arami (AA), Switzerland, has been the focus of heated debate since the proposal of Dobrzhinetskaya et al. (1996) of possible exhumation from greater than 300 km depth in the Earth's mantle, based primarily on evidence of abundant exsolution of $(Fe,Mg)TiO_3$ and chromite in olivine. The interpretation that very high pressures were necessary to account for the abundance of these oxides has been questioned on two different grounds: (1) evidence suggesting that the actual amount of TiO_2 present in AA olivine was overestimated by a factor of more than 20 (Hacker et al. 1997; Green et al. 1997a); and (2) argument that the titanate rods are not exsolution products but record breakdown of former lamellae of titanian clinohumite (Risold et al. 2001). Although additional evidence and arguments for and against exhumation from great depth also have been presented (Brenker and Brey 1997; Green et al. 1997b; 2000; Bozhilov et al. 1999; Arlt et al. 2000; Trommsdorff et al. 2000; Nimis and Trommsdorff 2001a, 2001b; Paquin and Altherr 2001a, 2001b; Dobrzhinetskaya et al. 2002), here we will only address evidence directly related to the question of the origin and significance of oxide inclusions in olivine.

Two generations of olivine are present in the AA peridotite. The older generation is coarse-grained, exhibits a lattice preferred orientation of olivine that has [100] normal to foliation (Möckel 1969), and the crystals contain abundant topotactically oriented inclusions of ilmenite and chromite (Dobrzhinetskaya et al. 1996). This generation has been recrystallized to varying degrees to a finer-grained aggregate (second generation) containing interstitial oxides. The abundance of rod-shaped inclusions of $(Fe,Mg)TiO_3$ contained within first-generation AA olivine was reported by Dobrzhinetskaya et al. (1996) to be >1 vol% (implying >0.6 wt% TiO_2), based upon digital image analysis of polished sections viewed in reflected light. Using a broad-beam microprobe technique, Hacker et al. (1997; see also response by Green et al. 1997a) analyzed a crystal of this material provided to them by the original authors and concluded that the integrated amount of TiO_2 in the olivine was only 0.02–0.03 wt%, even though Hacker confirmed the volume-fraction measurements of the original authors using backscattered electron imaging with a scanning electron microscope (Green et al. 1997a). This inconsistency might have been resolved had the inclusions been determined to have a much lower TiO_2 content than originally thought, but subsequent work has shown that all of the rods are ilmenite (Hacker et al. 1997; Green et al. 1997a; Risold et al. 2001), with no evidence of substitution of any element for Ti. Creating even greater confusion, the microprobe method of Hacker et al. (1997) returned the same low concentration of TiO_2 in a specimen of their own material for which the original authors measured a volume fraction of 0.02 vol% titanate, a value *consistent* with the microprobe measurements (Green et al. 1997a). It is clear, therefore, that the amount of TiO_2 present in olivine of the specimens of AA peridotite originally examined by Dobrzhinetskaya et al. (1996) remains to be characterized definitively.

We have revisited this subject by directly measuring the volume fraction of ilmenite in the cores of the oldest generation of olivine in selected specimens of the AA garnet lherzolite by applying confocal laser scanning microscopy (CLSM), as

* E-mail: bozhilov@citrus.ucr.edu

well as large-area chemical analysis with a scanning electron microscope (SEM) and an electron probe microanalyzer (EPMA). We find that both methods of analysis confirm the original abundances of ilmenite and TiO_2 reported by Dobrzhinetskaya et al. (1996). We then apply a stringent test of the models of origin of these oxides proposed by Dobrzhinetskaya et al. (1996) and by Risold et al. (2001), and find that the observations are consistent with the former model but inconsistent with the latter one.

METHODS

Confocal laser scanning microscopy (CLSM)

CLSM is a method that allows for precise three-dimensional imaging by optical sectioning (Sheppard and Shotton 1997). It is widely used in fluorescence mode for imaging of biological objects, but it also has been used in brightfield reflection mode for imaging of a wide variety of materials, including minerals (Petford and Miller 1992; Petford et al. 1995).

For this study, we utilized laser confocal system LSM510 (Carl Zeiss, Inc.) equipped with Ar ion and He(Ne) laser sources. The images were acquired in reflected laser light with 488 nm wavelength using a Zeiss Plan-Neofluar 100× oil immersion objective with numerical aperture of 1.3 and immersion oil with refractive index of 1.518 at room temperature. The experimental parameters theoretically allow lateral resolution of 150 nm and axial resolution of 438 nm. The samples were doubly polished petrographic thin sections of the Alpe Arami lherzolite mounted on standard glass slides by Petropoxy 154 (Palouse Petro Products). The thin sections were prepared in such a manner that for most grains the long axis of the rod-shaped ilmenite crystals, which is also parallel to the crystallographic **a** axis of ilmenite, was sub-parallel to the plane of the section. The dimensions of the individual ilmenite grains vary in the range of 0.2 to about 3 μm along the short axes, and from about 2 to 25 μm along their long axes (Figs. 1 and 2). More than 80 olivine grains in 5 petrographic thin sections from two localities, AA96 and AA73, were scanned, resulting in an image database of more than 5 GB. (See Appendix 1 for further discussion of the method, our procedures, and a detailed error analysis.)

The uncertainty in the volume determination of ilmenite in the AA olivine is ±37.52% (Appendix 1). This translates linearly into the estimated weight fraction of TiO_2 because the composition of the ilmenite crystals measured by EDX spectroscopy demonstrates that the Ti concentration is very close to its stoichiometric value of 1 atom per formula unit (apfu), with a relative error of about 5 wt% in the $(Mg,Fe)TiO_3$ formula of Alpe Arami ilmenite. This result, combined with the uncertainty in the volume determination, results in a total maximum error of ±42.52% in determining the weight fraction of TiO_2. The essence of this result is that the maximum possible error in our volume measurements is less than a factor of 2.

Large-area chemical analysis

Energy dispersive X-ray spectroscopy (EDS). Selected polished petrographic thin sections used to determine the volume fraction of ilmenite were analyzed in an FEI/Philips XL30-FEG SEM equipped with an EDAX EDS system and Si(Li) detector at the Central Facility for Advanced Microscopy and Microanalysis at the University of California, Riverside. The analyses and images were acquired at 15 kV accelerating voltage and 0.5 nA beam current. The spectra were collected by rapid scanning (~0.15 s per frame) of the focused electron beam

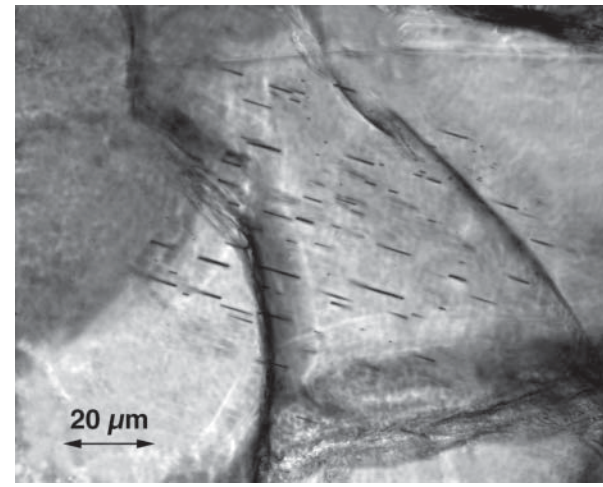

FIGURE 1. Optical micrograph (plane-polarized light) of an olivine crystal containing rod-shaped inclusions of ilmenite. The topotactically oriented ilmenite rods ($\langle 11\bar{2}0\rangle_{il}$ parallel to $[010]_{ol}$) are confined to the central part of the image and are surrounded by a border zone with essentially no inclusions.

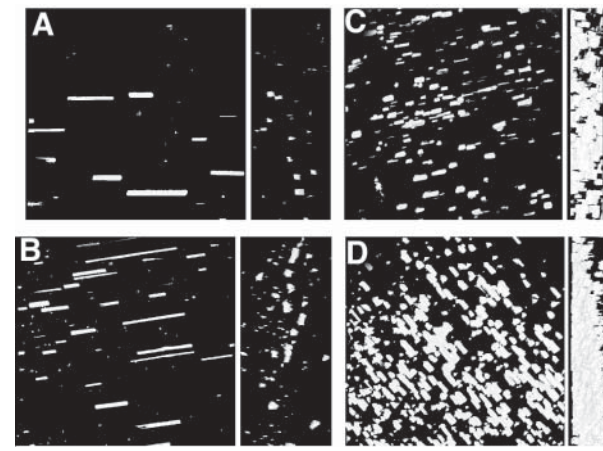

FIGURE 2. Confocal laser scanning micrographs of four olivine crystals with different concentrations of ilmenite (bright) inclusions: (**a**) 0.07 vol%, (**b**) 0.24 vol%, (**c**) 0.57 vol.%, and (**d**) 1.05 vol%. Each image represents a 20 μm-thick scanned volume of AA olivine and consists of a pair of images in which the left-hand side is a projection of the volume imaged along the microscope axis and the right-hand side is a projection after rotation of 90° around an axis lying in the thin section and oriented N-S in the figure. In the right-hand images, the microscope axis is oriented E-W in the figure. The vertical edge of each image is 92 μm.

over rectangular areas with dimensions ranging from 20×10 up to 60×30 μm in size. The spectra were collected for 200 s, at signal intensity of about 2000 cps, 20% dead time, and were reduced using the eDXi software v.2.31 from EDAX Inc. utilizing the ZAF correction procedure. The quantification was standardized using natural mineral standards of olivine, rutile and chromite, which were analyzed by scanning rectangular areas in the same manner as the sample. The volume fraction of ilmenite within the scanned areas was estimated based on back-scattered electron images and using an estimated sampling depth in olivine of 0.5 μm calculated as 0.3 of the Kanaya-Okayama range (Goldstein 1992).

Wavelength dispersive X-ray spectroscopy (WDS). To check the accuracy of the analyses obtained in the SEM by the EDS analysis, we studied one thin section by EPMA. Analyses were performed on a JEOL 733 Superprobe at the Analytical Facility of the Earth Sciences Division of the California Institute of Technology in Pasadena, CA. Spectra were collected by performing area scans in a similar manner to that applied in the EDS analyses. Experimental parameters were: 15 kV accelerating voltage, beam current of 25 nA, 0.2 μm beam size, intensity of 6000 cps for Si*K*α, acquisition time of 30 s per peak. Natural and synthetic standards of Ni-olivine, rutile, fayalite, forsterite, and Cr_2O_3 were used. Oxygen was calculated by cation stoichiometry and included in the matrix corrections. To verify the accuracy of the selected approach, spot analyses of the standard olivine and the sample were performed. Neither showed any statistically significant difference from the concentrations obtained using area scans.

RESULTS

In the first generation of AA olivine grains, ilmenite is distributed in interior zones as topotactically oriented rod-shaped inclusions (with $\langle 11\bar{2}0\rangle_{il}$ parallel to $[010]_{ol}$), generally surrounded by zones with few or no inclusions (Fig. 1). Within the high-density "cores" of these crystals, the distribution is typically highly homogeneous. CLSM (Fig. 2) shows that, despite the rigid parallelism of the ilmenite rods in individual crystals, their spatial distribution otherwise shows no apparent pattern. In particular, for the vast majority of olivine grains, the rods do not align into planes. However, in a small minority of crystals, the distribution is distinctly inhomogeneous, with concentrations occurring along (001) planes in the olivine structure (Fig. 3), closely resembling the "palisade" structure reported by Risold et al. (2001). We examined these planar structures with CLSM (Figs. 3a and 3b) and with conventional transmitted (Fig. 3c) and reflected (not shown) light microscopy. Both of these latter imaging modes showed that chromite platelets, although invisible in the CLSM images, are abundant among the ilmenite rods, just as they are in the more usual case when the ilmenite rods are distributed homogeneously (Dobrzhinetskaya et al. 1996).

The volumetric abundance of ilmenite measured directly by confocal microscopy in grains of several thin sections from each of two localities (AA96 and AA73) is shown in Figure 4. The average volume fraction of ilmenite in the cores of the older generation of olivine from these two different localities in the AA massif is 0.31%, which translates into 0.23 wt% TiO_2.

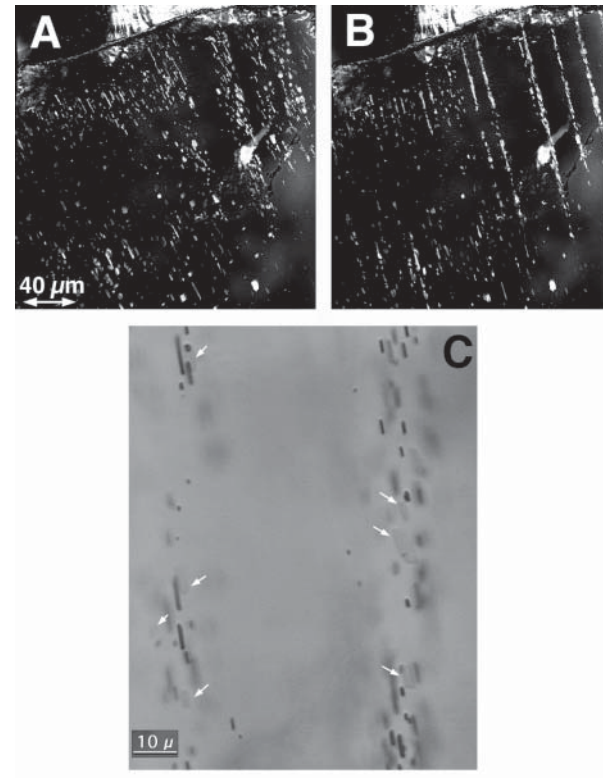

FIGURE 3. A pair of CLSM projection images (A, B) and conventional transmitted light optical micrograph of ilmenite grains (C) lying predominantly in (001) of olivine describing "palisade" structures. Image A is viewed along the microscope axis; image B has been rotated ~45° about an axis lying in the plane of the thin section and oriented N-S in the figure to demonstrate the planar alignment of the ilmenite crystals. Conventional optical microscopy (C) of this crystal shows chromite (white arrows) distributed amongst the "palisade" ilmenite in the same proportion as in crystals with homogeneous distribution of ilmenite (Dobrzhinetskaya et al. 1996).

The total maximal error in this determination is about 43% (relative) as discussed above, which translates into an absolute uncertainty in the average concentration of TiO_2 in the range of ±0.098 wt%.

During the complex geological history of the Alpe Arami massif, several metamorphic events are recorded, all of which could have caused redistribution of the mineral components. In particular, olivine of these rocks is variably recrystallized. The younger generation of olivine exhibits no oxide inclusions; as the new olivine crystals grew, the oxides were redistributed as discrete anhedral grains along olivine grain boundaries. Similarly, we found that the size and abundance of ilmenite rods in the first-generation crystals were systematically reduced in specimens that had suffered increasing degrees of serpentinization (Green et al. 1997a). These observations suggest that the maximum concentration of ilmenite now present is a more reliable indicator of the amount of TiO_2 originally incorporated into the olivine, but that even the maximum value likely provides only a lower bound. Our CLSM measurements

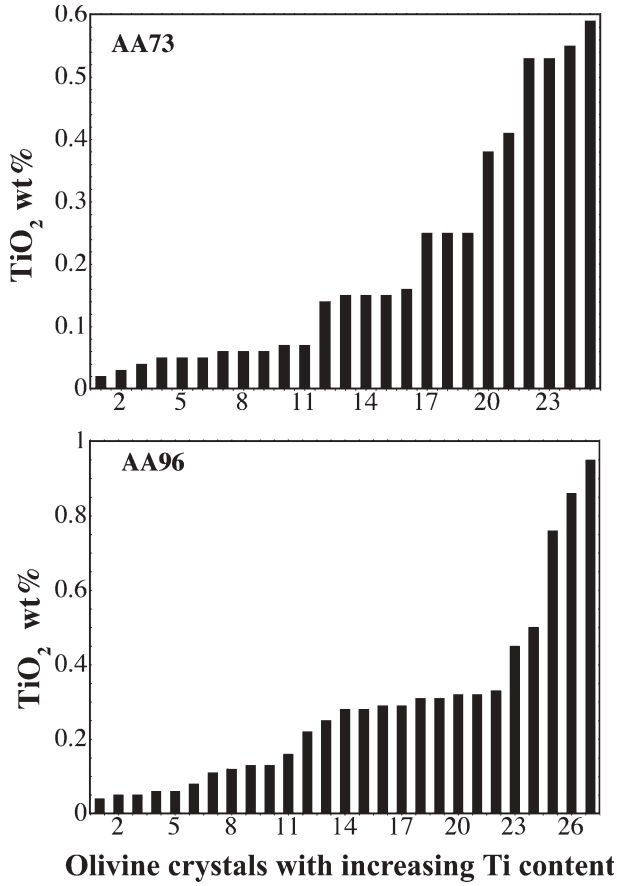

FIGURE 4. Wt% TiO_2 in two samples of AA olivine, AA73 and AA96, calculated from volume measurements of ilmenite abundance by CLSM.

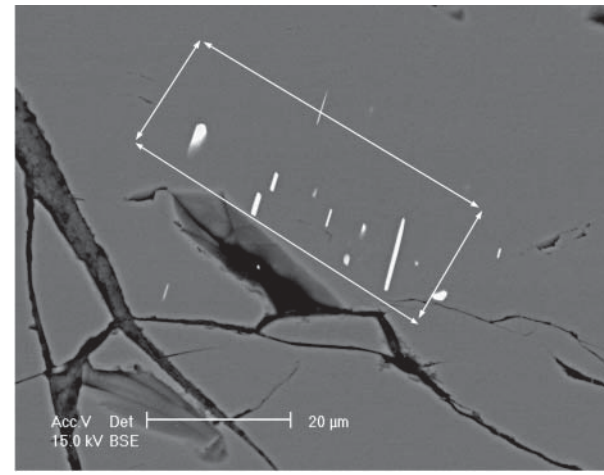

FIGURE 5. Back-scattered electron image of polished olivine grain of sample AA73 containing ilmenite and chromite inclusions (bright). The frame analyzed by EDX and WDX spectroscopy is outlined. Results of composition and area measurements are quantified in Table 1.

show a maximum volume fraction of ilmenite of 1.21%, corresponding to 0.9 ± 0.38 wt% TiO_2. Thus, even invoking the most conservative scenario (maximum error on the low side) reveals a concentration of TiO_2 in olivine of more than 10 times the maximum previously reported from olivine in xenoliths or peridotite massifs (Hervig et al. 1986). Thus, the original estimate of 1% maximum volume fraction (>0.6 wt% TiO_2) is on the conservative side of these statistics.

We also re-evaluated the correspondence between estimates of TiO_2 concentration by calculation from area-fraction measurements and direct measurements obtained by area scanning in the SEM and in the EPMA (Fig. 5 and Table 1). In contrast to Hacker et al. (1997), who employed a broad-beam technique that did not correlate well with their area measurements (see Green et al. 1997a), we found that scanning in either electron-beam instrument obtained TiO_2 concentrations closely similar to those calculated from area measurements.

DISCUSSION

The results presented here confirm the previous estimate of Dobrzhinetskaya et al. (1996) of >1 vol% $(Fe,Mg)TiO_3$ (>0.6 wt% TiO_2) in the cores of first-generation olivine grains from specimens of the Alpe Arami peridotite. The results also show that estimation of the area fraction of ilmenite by image analysis and subsequent calculation of wt% TiO_2 in the surface layer is consistent with large-area scanning analysis by SEM and EPMA. Moreover, our results demonstrate that whether ilmenite rods are distributed approximately homogeneously (the usual case in AA olivine) or concentrated into "palisades" lying in (001) planes, chromite plates are abundant.

The latter observation provides a test to distinguish between the two hypotheses that have been offered to explain the presence of ilmenite rods in olivine. In the original interpretation, Dobrzhinetskaya et al. (1996) proposed that the ilmenite components were originally dissolved in olivine and precipitated as topotactically oriented rods. Because the stoichiometry of olivine and ilmenite are different, this hypothesis requires the simultaneous precipitation of another phase. If the Ti had occupied octahedral sites in the olivine lattice, a silicate would have had to precipitate simultaneously (cf., Champness 1970) and if the Ti had been incorporated into the tetrahedral site, co-precipitation of an oxide would be required (cf., Green and Gueguen 1983, for an analogous example). These two alternatives are represented by Equations 1a and 1b, respectively:

$$Fe_4Ti\square Si_3O_{12} = FeTiO_3 + 3FeSiO_3 \quad (1a)$$

$$Fe_5(Cr,Fe,Al)_2\square Ti_4O_{16} = 4FeTiO_3 + Fe(Cr,Fe,Al)_2O_4 \quad (1b)$$

where □ signifies an octahedral vacancy in olivine and Mg can substitute for Fe. In contrast, Risold et al. (2001) proposed that the ilmenite rods have their origin in decomposition of atomic-scale hydrous layers of titanian clinohumite, which have previously been shown to form on (001) planes in olivine (Kitamura et al. 1987). In this case, the governing reaction is:

$$Fe_{17}TiSi_8O_{34}(OH)_2 = 8Fe_2SiO_4 + FeTiO_3 + H_2O \quad (2)$$

where, again, Mg can substitute for Fe. Risold et al. (2001) assumed that the olivine produced in this reaction was "plated" onto the host olivine and H_2O escaped to the grain boundaries. Note that the exsolution hypothesis requires the presence of two solid product phases with complementary chemistry and a specified abundance ratio. The presence of chromite in a volumetric ratio to ilmenite of approximately 1:4–1:5 (Dobrzhinetskaya et al. 1996) is consistent with Equation 1b. Additional supporting evidence is the growth of enstatite crystals accompanying dissolution of TiO_2 in olivine during the experiments of Dobrzhinetskaya et al. (2000), which is consistent with tetrahedral occupancy of Ti in olivine. However, the titanian clinohumite hypothesis requires the absence of additional phases, hence the presence of chromite and its abundance would have to be explained by ad hoc arguments.

An additional, independent, difficulty with the hypothesis of Risold et al. (2001) is that bulk crystals of titanian clinohumite have never been found in samples of Alpe Arami garnet peridotite, nor have the characteristic olivine-ilmenite symplectites that mark the previous presence of that mineral (Möckel 1969; Green et al. 1997b). With the much larger abundance of ilmenite now confirmed here for AA olivine, the lack of bulk titanian clinohumite or evidence for its previous existence in this massif makes application of the hypothesis of Risold et al. (2001) significantly less reasonable. It would require the spacing of the postulated clinohumite defects to be approximately 10 nm (~20 unit cells) rather than the 520 nm proposed in their paper or the 30 μm (30 000 nm) observed above (Fig. 3).

Two important additional pieces of information relevant to this puzzle have been added recently: (1) Explanation of the rod morphology of ilmenite in olivine. Whereas Dobrzhinetskaya et al. (1996) argued that ilmenite precipitates in olivine should have a platy habit, based upon comparison of the lattice spacings of $FeTiO_3$ ilmenite and those of olivine, Risold et al. (2001) pointed out that ilmenite with a significant geikielite component ($MgTiO_3$) would be expected to exhibit rod morphology with $\langle 11\bar{2}0\rangle$ ilmenite parallel to [010] of olivine as observed. The fact that significant Mg substitution for Fe in ilmenite is to be expected at high pressures strongly suggests that this is the probable explanation for the rod morphology. (2) Explanation of the preferred orientation of olivine observed in the older generation of AA olivine. Jung and Karato (2001) conducted deformation experiments on olivine under conditions of relatively high f_{H_2O} and found that the lattice preferred orientation (LPO) expected under such conditions would have [100] subnormal to the foliation and [001] subparallel to the lineation – the same LPO as observed for the older generation of olivine in AA. This flow regime would also naturally yield (001) kink-band boundaries (Zeuch and Green 1984) on which exsolving oxides could nucleate preferentially (Green and Gueguen 1983). The experiments of Jung and Karato (2001) were conducted on H_2O-saturated olivine at pressures of approximately 2–2.5 GPa; higher pressures would provide similar or higher f_{H_2O} with lesser amounts of H_2O present because at constant composition, f_{H_2O} increases with pressure and so does the solubility of H_2O in olivine (Mie and Kohlstedt 2000). These observations strongly suggest that first-generation AA olivine attained its LPO under conditions of enhanced H_2O solubility whereas second-generation AA olivine (which exhibits "normal" olivine LPO with [010] subnormal to foliation and [100] subparallel to lineation; Möckel 1969; Buiskool Toxopeus 1976, 1977) was generated and deformed under low H_2O solubility. In turn, this interpretation implies that first-generation olivine was deformed at temperatures above the stability field of titanian clinohumite (Ulmer and Trommsdorff 1999; see also Stalder and Ulmer 2001). Such conditions are consistent with the lack of bulk titanian clinohumite in AA peridotite, and the conditions of origin we previously estimated (Dobrzhinetskaya et al. 1996; Bozhilov et al. 1999; Green et al. 2000), and would be compatible with exsolution of small quantities of titanian clinohumite if physical conditions changed so as to make the latter stable (consistent with rare hydrous defects of the clinohumite type reported by Risold et al. (2001). Our interpretation does not match directly any of the various *P-T* conditions established by other workers, but it is perfectly consistent with the data obtained from thermobarometry by Ernst (1981), Medaris and Carswell (1990), Brenker and Brey (1997), and Paquin and Altherr (2001a). The fact that these latter studies record significantly lower pressure and temperature is most probably due to the fact that the cation distribution among the various minerals present during the peak metamorphic event was not arrested in the respective phases, and many of the components remained mobile. As a consequence, thermobarometry measurements can provide only partial information involving mostly later stages of the evolution of this lherzolite body.

These observations, taken together, are consistent with origin of the AA peridotite under hydrous conditions where solubility of TiO_2 in olivine exceeded 0.6 wt%, i.e., at pressures of 9–12 GPa, depending on temperature (Dobrzhinetskaya et al. 2000; Tinker and Lesher 2001), conditions where Ti apparently can be accommodated into the tetrahedral site of olivine. Subsequent decompression to lower pressures would result in exsolution of ilmenite and chromite, and attainment of conditions in which H_2O solubility in olivine was reduced sufficiently so that recrystallization and deformation occurred by nominally anhydrous processes (although perhaps contemporaneously with hydrous metamorphism). The titanian clinohumite breakdown hypothesis fails to explain: (1) the generally homogeneous distribution of ilmenite in first-generation AA oli-

TABLE 1. Comparison of ilmenite distribution determined by EDS, WDS, and area measurements*

	EDS-SEM	WDS -EPMA	Area
SiO_2	39.81	39.38	
TiO_2	1.35	1.41	
MgO	49.04	48.07	
FeO	8.9	10.31	
NiO	0.28	0.41	
Cr_2O_3	0.62	0.36	
Total	100.00	99.94	
Scanned frame	45 ×15 μm	3 frames of 15 ×15 μm	675 μm²
Olivine	98.032	97.915	97.6%
Ilmenite	1.666	1.735	
Chromite	0.302	0.350	
Ilmenite + Chromite	1.968	2.085%	2.4%

* Oxide concentrations and calculated mineral proportions in wt%.

vine; (2) the appearance of chromite wherever ilmenite is found (in amounts predicted by the exsolution hypothesis), even within "palisades," and (3) the lack of bulk crystals of titanian clinohumite in AA peridotite.

It is important to emphasize here that the incompatibility of the Risold et al. hypothesis with the observations for the AA peridotite does not necessarily invalidate that hypothesis for the other two Alpine peridotites for which it has been advanced. We have no personal knowledge of either of these peridotites, it could be that the Cima di Gagnone (CDG) and Monte Duria (MD) peridotites have a significantly different history, quite possibly not including a very-high-pressure chapter. For example, in the images of Risold et al. (2001) from CDG and MD samples, it is clear that a large fraction of ilmenite rods lie in "palisades," whereas their image of AA shows the rods to be more broadly distributed. Such contrasts are consistent with the geochemical results of Paquin et al. (2001), showing that AA is distinctly different from CDG. In particular, the data (as we understand them) are consistent with CDG being a subducted serpentinite that has been subjected to moderately high-pressure metamorphism, whereas AA is a mantle peridotite that shows no evidence of a shallow hydrous history prior to its alteration late in the alpine orogeny.

Lastly, given that CDG, MD, and AA all lie in the Cima Lunga unit of the Lepontine nappe, it is probable that the three peridotites share a common history late in the exhumation process. If our interpretation of the LPO of olivine of the older generation in AA is correct, then the water dissolved in the olivine during deformation at very high pressure would be expected to precipitate as titanian clinohumite lamellae if, during exhumation, the AA peridotite entered the stability field of titanian clinohumite. The exhumation curve of Brenker and Brey (1997) suggests that such entry into the titanian clinohumite field did occur. The late, low-pressure, heating event that was also recorded by Brenker and Brey (1997) would later cause breakdown of those lamellae and they could form a small number of palisades in AA olivine (as well as breakdown of bulk titanian clinohumite and formation of palisades in CDG and MD).

ACKNOWLEDGMENTS

We thank Chi Ma for extensive and careful calibration of the EPMA at the Earth Sciences Division of the California Institute of Technology and assistance with the beam scanning experiments with that instrument. We also thank Adrian Brearley, Gary Ernst, and an anonymous reviewer for their critical reviews and helpful comments that led to improvement of the paper.

REFERENCES CITED

Arlt, T., Kunz, M., Stolz, J., Armbruster, T., and Angel, R.J. (2000) P-T-X data on $P2_1/c$- clinopyroxenes and their displacive phase transitions. Contributions to Mineralogy and Petrology, 138, 35–45.

Bozhilov, K.N., Green, H.W. II, and Dobrzhinetskaya, L. (1999) High-pressure clinoenstatite in the Alpe Arami peridotite. Science, 284, 128–132.

Brenker, F.E. and Brey, G.P. (1997) Reconstruction of the exhumation path of the Alpe Arami garnet-peridotite body from depths exceeding 160 km. Journal of Metamorphic Geology, 15, 581–592.

Buiskool Toxopeus, J.M.A. (1976) Petrofabrics, microstructures and dislocation substructures of olivine in peridotite mylonite (Alpe Arami, Switzerland). Leidse Geologische Mededelingen, 51, 1–36.

——— (1977) Deformation and recrystallization of olivine during mono- and polyphase deformation. A transmission electron microscope study. Neues Jahrbuch für Mineralogie Abhandlungen, 129, 233–268.

Champness, P.E. (1970) Nucleation and growth of iron oxides in olivines, $(Mg,Fe)_2SiO_4$. Mineralogical Magazine, 37, 790–800.

Dobrzhinetskaya, L.F., Green, H.W. II, and Wang, S. (1996) Alpe Arami: a peridotite massif from depths of more than 300 kilometers. Science, 271, 1841–1845.

Dobrzhinetskaya, L., Bozhilov, K.N., and Green, H.W. II. (2000) The solubility of TiO_2 in olivine: Implications for the mantle wedge environment. Chemical Geology, 163, 325–338.

Dobrzhinetskaya, L.F., Schweinehage, R., Massonne, H.-J., and Green, H.W. II. (2002) Silica precipitates in omphacite from eclogite at Alpe Arami, Switzerland: Evidence of deep subduction. Journal of Metamorphic Geology, 20, 481–592.

Ernst, W.G. (1981) Petrogenesis of eclogites and peridotites from the Western and Ligurian Alps. American Mineralogist, 66, 443–472.

Goldstein, Joseph. I., Ed. (1992) Scanning electron microscopy and X-ray microanalysis: a text for biologists, materials scientists, and geologists. (2nd edition), 820 p. Plenum Press, New York.

Green, H.W. II and Gueguen, Y. (1983) Deformation of peridotite in the mantle and extraction by kimberlite: A case history documented by fluid and solid precipitates in olivine. Tectonophysics, 92, 71–92.

Green, H.W. II, Dobrzhinetskaya, L., and Bozhilov, K. (1997a). Determining the origin of ultra-high pressure lherzolites. (response), Science, 278, 704–707.

Green, H.W. II, Dobrzhinetskaya, L., Riggs, E., and Jin, Z.-M. (1997b) Alpe Arami: A peridotite massif from the mantle transition zone? Tectonophysics, 279, 1–21.

Green, H.W. II, Dobrzhinetskaya, L.F., and Bozhilov, K.N. (2000) Mineralogical and experimental evidence for very deep exhumation from subduction zones. Journal of Geodynamics, 30, 61–76.

Hacker, B.R., Sharp, T., Zhang, R.Y., Liou, J.G., and Hervig, R.L. (1997) Determining the origin of ultrahigh-pressure lherzolites. (discussion) Science, 278, 702–704.

Hervig, R.L., Smith, J.V., and Dawson, J.B. (1986) Lherzolite xenoliths in kimberlites and basalts: Petrogenetic and crystallochemical significance of some minor and trace elements in olivine, pyroxenes, garnets and spinel. Royal Society of Edinburgh Transactions, Earth Sciences, 77, 181–201.

Jung, H. and Karato, S. (2001) Water-induced fabric transitions in olivine. Science, 293, 1460–1463.

Kitamura, M., Kondoh, S., Morimoto, N., Miller, G.H., Rossman, G.R., and Putnis, A. (1987) Planar OH-bearing defects in mantle olivine. Nature, 328, 143–145.

Medaris, L.G. and Carswell, D.A. (1990) The petrogenesis of Mg-Cr garnet peridotites in European metamorphic belts. In D.A. Carswell, Ed., Eclogite facies rocks, 260–290. Blackie, Glasgow.

Mei, S. and Kohlstedt D.L. (2000) Influence of water on plastic deformation of olivine aggregates 2. Dislocation creep regime. Journal of Geophysical Research, 105, 21471–21481.

Möckel, J.R. (1969) Structural petrology of the garnet peridotite of Alpe Arami (Ticino, Switzerland). Leidse Geologische Mededelingen, 42, 61–130.

Nimis, P. and Trommsdorff, V. (2001a) Revised thermobarometry of Alpe Arami and other garnet peridotites from the Central Alps. Journal of Petrology, 42, 103–115

——— (2001b) Comment on "New constraints on the P-T evolution of the Alpe Arami garnet peridotite body (Central Alps, Switzerland)" by Paquin and Altherr (2001). Journal of Petrology, 42, 1773–1779.

Paquin, J. and Altherr, R. (2001a) New constraints on the P-T evolution of the Alpe Arami garnet peridotite body (Central Alps, Switzerland). Journal of Petrology, 42, 1119–1140.

——— (2001b) "New constraints on the P-T evolution of the Alpe Arami garnet peridotite body (Central Alps, Switzerland)": Reply to comment by Nimis and Trommsdorff (2001). Journal of Petrology, 42, 1781–1787.

Paquin, J., Olker, B., Altherr, R., and Vennemann, T.W. (2001). Trace element partitioning in orogenic garnet peridotites from the central alps (Switzerland) and western gneiss region (Norway). Abstract #3230. LPI Contribution No. 1088, Lunar and Planetary Institute, Houston (CD-ROM).

Petford, N. and Miller, J.A. (1992) Three-dimensional imaging of fission tracks using confocal scanning laser microscopy. American Mineralogist, 77, 529–33.

Petford, N., Miller, J.A., and Rankin, A.H. (1995) Preliminary confocal scanning laser microscopy study of fluid inclusions in quartz. Journal of Microscopy, 178, 37–41.

Risold, A.-C., Trommsdorff, V., and Grobety, B. (2001) Genesis of ilmenite rods and palisades along humite-type defects in olivine from Alpe Arami. Contributions to Mineralogy and Petrology, 140, 619–628.

Sheppard, C.J.R. and Shotton, D.M. (1997) Confocal laser scanning microscopy, 106 p., Oxford: BIOS Scientific; New York, Springer, in association with the Royal Microscopical Society.

Stalder, R. and Ulmer, P. (2001) Phase relations of a serpentine composition between 5 and 14 GPa: significance of clinohumite and phase E as water carriers into the transition zone. Contributions to Mineralogy and Petrology. 140, 670–679.

Tinker, D. and Lesher, C.E. (2001) Solubility of TiO_2 in olivine form 1 to 8 GPa. EOS Transactions of the American Geophysical Union 82, Fall Meet. Supplement, Abs #V51B-1001.

Trommsdorff, V., Hermann, J., Müntener, O., Pfiffner, M., and Risold, A.C. (2000) Geodynamic cycles of subcontinental lithosphere in the Central Alps and the

Arami enigma. Journal of Geodynamics, 30, 77–92.
Ulmer, P. and Trommsdorff, V. (1999) Phase relations of hydrous mantle subducting to 300 km. In Y. Fei et al., Eds, Mantle Petrology: Field Observations and High Pressure Experimentation: A Tribute to Francis R. (Joe) Boyd, Geochemical Society. Special Publication, 6, 259–281.
Zeuch, D. H. and Green, H. W., II. (1984) Experimental deformation of a synthetic dunite at high temperature and pressure. Part II: Transmission electron microscopy. Tectonophysics, 110, 263–296.

MANUSCRIPT RECEIVED APRIL 2, 2002
MANUSCRIPT ACCEPTED DECEMBER 2, 2002
MANUSCRIPT HANDLED BY ADRIAN BREARLEY

APPENDIX 1. PROCEDURE FOR ILMENITE VOLUME DETERMINATION BY CONFOCAL LASER SCANNING MICROSCOPY

CLSM is a method that allows for precise three-dimensional imaging by optical sectioning. Laser light is focused by an objective lens onto the object, and the reflected or fluorescent light is focused onto a photodetector via a beam splitter. A confocal aperture (called a pinhole) is placed in front of the detector. Because the pinhole and the focal point inside the specimen are confocal, the only light that can pass through the pinhole and be registered by the detector is that coming from the focal point. The result is a high-definition image of the focal point, which is largely free of stray light, in contrast to that of conventional light microscopy (Sheppard and Shotton 1997). By scanning of the focused spot relative to the object, a 2D image with an extremely shallow depth of field is built up and the generated digital image is stored in a computer imaging system. By consecutively changing the depth of the focal plane within the specimen, a series of optical sections of an object can be obtained, which then can be combined into a 3D image that is in focus at all levels. The thickness of each optical section is a function of the pinhole diameter and the wavelength of the laser light. The 3D reconstructions were created by scanning volumes with total depths of 10 to 20 μm and lateral dimensions from 90 × 90 to 130 × 130 μm. Each volume was imaged by collecting a series of consecutive optical slices. The thickness of an individual optical slice was 250 nm determined in accordance with Nyquist's theorem, which requires that consecutive sections overlap optically. Each volume is built up by combining into Z-series fifty to eighty individual optical slices, using the LSM software version 2.5 by Zeiss Inc.

The volume of ilmenite in each optical section was determined by separating the objects from the background on the basis of their intensity values. In an 8-bit image, there are 256 levels of gray, where white = 255 and black = 0. Because olivine is transparent, it does not introduce any measurable intensity in the image acquired in reflectance, and creates a flat black background with values of intensity of around 0 but not higher than 10. The strongly reflecting ilmenite crystals are the only opaque phase in the olivine grains (Figs. 1 and 2), which enables us to separate them quite easily from the olivine background by defining a threshold of 100 (we specifically investigated whether the very thin, almost transparent, chromite lamellae in these sections were visible or not in the CLSM images; they were not). The number of pixels in each image with intensity more than 100 was converted into an area fraction. By cutting out the intensities below 100, weak reflections due to refraction and scattering are almost eliminated. The volume fraction of ilmenite in an optical slice was calculated by multiplying the area of ilmenite by 0.25 μm, the thickness of the slice. The volume fractions for each slice were added together to give the total volume fraction of ilmenite in the scanned volume of olivine.

The dimensions of the ilmenite rods along the Z-axis are overestimated during the measurement in the confocal microscope. This is due to over-sampling, lower resolution along the optical axis (Z-axis), and very small dimensions of the crystals along the microscope Z-axis. To address this problem, a correction factor was introduced, which is determined by measuring the dimensions of the rod-shaped ilmenite crystals in a plane perpendicular to their longest axis. First, we measured a limited number of olivine grains where the long axis of the ilmenite rods is oriented almost perpendicular to the plane of the thin-section. All ilmenite crystals measured in such a manner show approximately equidimensional cross-sections perpendicular to their long axis. This observation was incorporated into the correction factor for determining the volume of ilmenite in the 3D optical sections. It was accomplished by creating 3D digital reconstructions of the imaged olivine slabs and the enclosed ilmenite rods. These 3D slabs were rotated digitally so that the long axes of the ilmenite rods align perpendicular to the plane of view. In such an orientation, it is possible to measure directly the cross-section perpendicular to the long axis of the ilmenite crystals. In contrast to the ilmenite rods visualized directly in cross-section perpendicular to the long axis, the ilmenite rods in general orientation show rectangular cross-sections, where the longer side is always parallel to the optic axis of the microscope during the original image acquisition. Such an elongation is caused by artificial stretching of the images of the ilmenite crystals parallel to the optic axis due to the oversampling and poorer resolution along the microscope Z-axis, as discussed above. Since the ilmenite crystals have almost equidimensional cross-sections perpendicular to their long axis as determined from direct observations, and the vast majority of the imaged ilmenite crystals were oriented with their long axis almost perpendicular to the optic axis, a correction factor was introduced for the third dimension of ilmenite rods, which was perpendicular to the optic axis during image acquisition.

The correction factor was determined by digitally tilting the ilmenite crystals so that their long axes align perpendicular to the plane of view and by consequent measuring and dividing the long by the short side in cross-section perpendicular to the long axis. For each set of optical sections, about 15 ilmenite rods were measured to determine the correction factor. There were slight variations among the correction factors determined for individual grains, but all are close to 2.

The originally determined volume in a given crystal was adjusted by dividing it by the specific correction factor determined for that crystal. The accuracy of this correction scheme was checked by determining the variation of the cross-section of ilmenite crystals perpendicular to the long axis. About 30 individual ilmenite crystals were measured and the ratio of the lengths of the two measured sides is 1.01, with a standard deviation of 12%, which can be accepted as the maximum error in determining the correction factor. The error in determination of the volume fraction was estimated by taking into ac-

count the uncertainty of size determination due to the limits of the lateral resolution and the error in determination of the correction factor. By using the values of the average size of the ilmenite crystals (width 1.32 μm, length 5.51 μm), the maximum error in volume determination due to inaccurate size measurement caused by the limited resolution was calculated as a sum of the errors in measuring the lateral dimensions. With lateral resolution of ±150 nm, the average error for measuring the width of ilmenite rods amounts to 11.40% and the error in measuring the length is 2.72%. The resolution along the optical axis is ±438 nm, which results in an average error of measurements along the Z-axis of 33%. By introducing the correction factor, this error is minimized to the error of uncertainty in measuring the lateral width of the ilmenite rods, which is 11.40% plus the 12% error in determining the correction factor or 23.40%. Thus the total maximum error is the sum of the errors in measuring the width and length of ilmenite crystals (11.40 + 2.72 = 14.12%) plus the error of uncertainty in determining the third dimension of ilmenite (23.4%), which sums to 37.52%.